Diffuse Gamma-Ray and Neutrino Emission from the Local Supercluster

Tanja M. Kneiske*, Jörg Kulbartz†, Dieter Horns* and Günter Sigl †

*Institut für Experimentalphysik, Universität Hamburg, Luruper Chaussee 149, 22761 Hamburg
†II. Institut für theoretische Physik, Universität Hamburg, Luruper Chaussee 149, 22761 Hamburg

***Abstract*. The formation and evolution of galaxies in the local Supercluster have very likely lead to the acceleration of energetic particles by individual galaxies as well as in large scale shocks in merger events. Here, we investigate the signatures of cosmic-rays up to energies of a few 10^{19} eV which are efficiently confined in the intra-cluster medium. Subsequent photo-pion production and pair-production/inverse Compton cascades lead to a large-scale anisotropy at TeV and EeV-energies along the super-galactic plane. Additionally, energetic neutrinos are produced. We provide predictions and discuss implications for the cosmic-ray energy density in the local Supercluster.**

***Keywords*: Diffuse emission, Cosmic Rays, Local Supercluster**

I. Introduction

Very recently the AUGER experiment claimed a statistically significant coincidence between the arrival direction of the highest energy ($E > 10^{19}$ eV) cosmic-ray events and nearby active galactic nuclei coarsely aligned with the super-galactic plane [1]. Given the over-density of galaxies in the Supercluster it appears feasible that cosmic-ray acceleration and confinement leads to an enhanced cosmic ray energy density within the local Supercluster (LSC) and, therefore, also at the position of the Milky Way. The presence of sufficiently energetic cosmic-rays in the environment of the LSC will lead to interactions with ambient diffuse photon fields like the cosmic microwave background (CMB) but also with the metagalactic radiation field (MRF) and the LSC radiation field (SRF). Pion photo-production leads to the injection of secondary particles like electrons, neutrinos, and high-energy photons which subsequently undergo photon-photon pair-production and Inverse-Compton scattering leading to electromagnetic cascades. The result is a high energy gamma-ray flux from the super-galactic plane with two broad maxima around 10^{12} and 10^{19} eV, respectively. A detection of the ultra high energy photon flux with the Pierre Auger observatory can be used to determine the cosmic-ray energy density in the LSC.

II. Cosmic Ray Propagation

A. Cosmic ray spectrum

In the following we will assume for the sake of simplicity a pure proton composition.[1] The energy distribution of protons has been chosen to be a power-law with an exponential cut-off. The power-law slope α, exponential cut-off energy E_c, and the normalization are in principle free parameters. Without favoring a specific acceleration mechanism, we use the power-law slope measured by AUGER of $\alpha \approx 2.7$ for proton energies $E_p \geq E_{\rm min} = 10^{17}$eV and $E_c = 4 \times 10^{19}$ eV. Keeping the slope fixed, we consider two limiting scenarios for the normalization. As a conservative, lower limit for the normalization, we use the cosmic-ray spectrum above 10^{19} eV as observed by AUGER and thus at Earth (scenario A). In a second scenario B we envisage that the cosmic ray flux in the central regions of the LSC may be higher than at Earth due to partial confinement around regions of enhanced source activity. In this scenario the maximal possible enhancement is still constrained by upper limits on the photon fraction from AUGER observations.

In the following, we will focus on results for these specific parameters discussed above. A more in-depth discussion of photon and neutrino spectra with different proton spectra will be presented elsewhere.

B. Cosmic-ray propagation

Propagation of cosmic rays in the Supercluster medium has been modeled using the results obtained by [2], where they derived a diffusion coefficient $D(E)$ for an extragalactic turbulent magnetic field. They assume a Kolmogorov-like turbulence with principal scale $\lambda_{\rm max} = 1$ Mpc and a field variance of $\sqrt{\|\mathbf{B}^2\|} = 10$ nG. The components of the field are distributed over a Gaussian of mean zero, and the coherence length $\lambda_c \simeq \lambda_{\rm max}/5 \simeq 0.2$ Mpc.

Based upon this (isotropic) diffusion coefficient, the escape time scales for leaving the super-cluster volume, can been estimated using the relation

$$\tau_{\rm esc} = \frac{R^2}{2D(E)}. \quad (1)$$

[1]The effect of heavier nuclei propagation will be presented elsewhere.

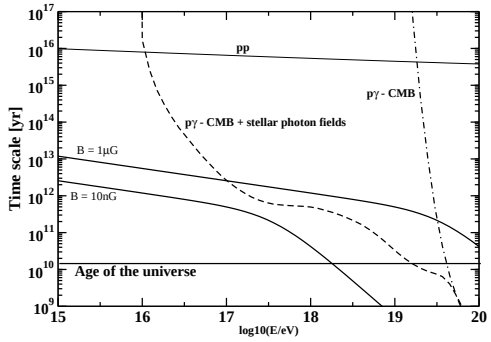

Fig. 1. Times scales as a function of proton energy. Thick solid lines show the escape time of protons due to diffusion in the LSC central regions for two magnetic field strength and a diameter of 25 Mpc. The energy loss time for proton-proton interaction (for a gas density of $n = 10^{-8}$ cm^{-3}) is shown as thin solid line, while the energy loss time for proton-photon interaction is plotted as dashed and dot-dashed line for the total diffuse photon fields and CMB photons only, respectively.

C. Energy-losses

Energy-losses due to interaction with ambient photons and interstellar gas have been studied as well[2]. The energy loss time scale is approximated by

$$\tau_{\rm loss} = \frac{E_p}{\left|\dot{E}_p\right|}. \qquad (2)$$

The resulting energy loss time scales, together with the estimated escape time, are presented in Fig. 1.

Three conclusions can be drawn from figure 1. First, cosmic rays up to the highest energies of $E = 10^{19} \ldots 10^{20}$ eV can be trapped in the LSC volume on time scales in the same order as the age of the universe, provided the magnetic fields are larger than about 10 nG. This justifies the possibility of scenario B in which the cosmic ray flux in the central LSC regions is considerably higher than at Earth due to a higher source activity.

Second, hadronic interactions are negligible for proton energy loss, due to the small gas density in the inter-cluster medium for which a number density of 10^{-8} cm^{-3} has been chosen. This number is motivated by the assumption that the missing baryonic matter in the universe exists in the form of the so called warm/hot medium which would be distributed in the large scale structure filling 10%-25% of the universe. An evenly distributed gas in the universe would lead to even lower gas densities.

Third, adding stellar radiation fields to the cosmic microwave background is essential. It leads to significant energy loss between 10^{16} eV and 10^{19} eV. The photon fields used are described in more detail in the next section.

The three points can be summarized to a high efficiency of trapped protons with energies between 10^{17} eV and 10^{19} eV in producing secondaries due to photon-meson interaction.

[2]We neglect energy losses due to adiabatic expansion as well as due to pair-production processes.

III. The low energy diffuse photon fields

In the LSC three kinds of photon fields are presents. The universal cosmic microwave background is constant in the Supercluster volume and only changing over cosmological distances. It can be easily expressed by a black body spectrum with a temperature of 2.7 K. A second photon field, which can also be assumed constant on small scales, is the extragalactic radiation field. It is produced by galaxies outside the LSC which are too far away for being important as single sources. This photon field has been included using a model presented in [3]. The third radiation field is a LSC photon field produced by the ten thousand galaxies in the Supercluster. The optical to infrared emission produced by these galaxies can escape the cluster medium, which basically consists of gas, having almost no influence on the non ionizing stellar emission. These photons form a photon field between galaxy clusters, which can be simply added to the already discussed stellar and cosmic microwave backgrounds. Here we assume as a first approximation that the luminosity is distributed homogeneously throughout a cylindrical Supercluster with a radius of $R = 25$ Mpc and a height of $H = 10$ Mpc. The modeling of the diffuse emission of the LSC has been done similar to [3]. The evolution of the local Supercluster and the average quantities can be assumed to follow cosmic behavior, because of its large dimensions. The number of galaxies is assumed to be ten thousand with a star formation rate of each galaxy $\dot{\rho}_{\rm gal} = 7$ M$_\odot$ yr^{-1}. The differential luminosity as a function of photon energy can be obtained from a simple stellar population for a chosen metalicity and initial mass function. The effects of dust and gas on the stellar emission has been included as in [3]. The LSC-star-formation-rate (LSC-SFR) $\dot{\rho}_\star(z)$ is chosen to follow the global star formation rate. The total star formation rate is

$$\dot{\rho}_\star = \frac{\dot{\rho}_{\rm gal} N_{\rm gal}}{H \pi R^2} \qquad [{\rm M}_\odot {\rm yr}^{-1} {\rm Mpc}^{-3}]. \qquad (3)$$

The convolution integral is

$$\epsilon(\lambda) = \int_{0.01}^{5} L_{\rm gal}(\lambda) \dot{\rho}_\star(z) \frac{dt}{dz} dz \qquad (4)$$

The emissivity is calculated at a redshift of 0.01 which is about 50 Mpc away from Earth. Since the redshift is only important for stellar evolution changing this value does not influence the result significantly. The flux is calculated for a certain point in the LSC by integrating the emissivity over the volume of the cylinder. Assuming a constant emissivity the resulting flux can be approximated to be constant in the LSC. The photon flux is independent of the angle and only weakly changing within a radius of $r \approx 20$ Mpc, which is the location of our galaxy. We can therefore add up the three radiation fields shown in figure 2.

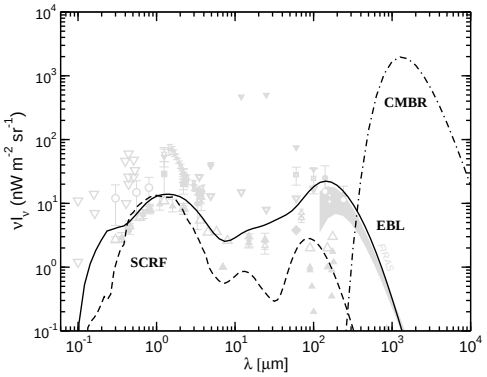

Fig. 2. Low energy diffuse photon fields in the LSC. Shown is the cosmic microwave background (dot-dashed line), the extragalactic background light (solid line; see Ref.[3]) and the Supercluster photon field (dashed line).

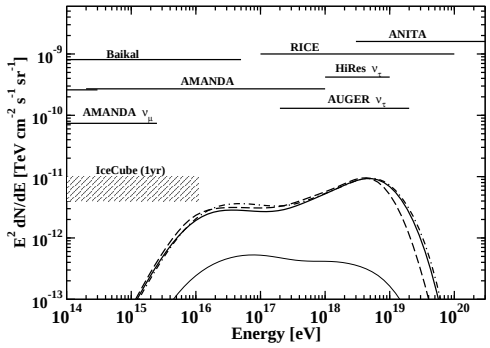

Fig. 3. Diffuse neutrino flux from the local Supercluster for scenario B for different neutrinos flavors (solid lines are electron (anti) neutrinos, dashed (dot-dashed) lines are myon (anti) neutrinos). The effect of neutrino oscillation has not been taken into account. The limits are taken from [15]. Green limits are for all neutrino flavors, while the blue AMANDA limit is for electron neutrinos only and the violet HiRes and AUGER limit are only for tau neutrinos.

A good test for the LSC radiation field is to compare the luminosity density at 2 micron with observed values which is about 4.1×10^8 $M_\odot$ Mpc^{-3} from the 2dF survey [4] or 4.21×10^8 $M_\odot$ Mpc^{-3} from 2MASS and SDSS [5]. The value in the calculation above is about a factor of 2 higher than these values. It is still a realistic result given the fact that the observed data are derived for the total sky, mostly excluding regions of the local large scale structure. The emissivity from the region of the super-galactic plane could therefore be higher. A more detailed discussion on the uncertainties will be done elsewhere.

IV. High energy diffuse backgrounds

The secondary particle spectra from photon-proton interaction have been calculated using the parameterization suggested by [6]. It is important to notice that the protons and the photons are distributed isotropically. The energy of the photon ϵ and the energy of the proton E_p have to fulfill $\epsilon << m_\pi$ and $E_p << m_p$, where $m_\pi (= m_\pi^0 = m_\pi^+)$ and m_p is the mass of the meson and the mass of the proton, respectively. The production of e.g. gamma-rays from photo-pion production and decays of $\pi^0 \rightarrow \gamma\gamma$ in the energy interval $(E_\gamma, E_\gamma + dE\gamma)$ per second per cm^3 is given by

$$\frac{dN}{dE_\gamma} = \int\int f_p(E_p) f_{\rm ph}(\epsilon) \phi_\gamma \left(\frac{4\epsilon E_p}{m_p^2}, \frac{E_\gamma}{E_p} \right) \frac{dE_p}{E_p} d\epsilon \quad (5)$$

where $f_p(E_p)$ is the proton spectrum described above, $f_{\rm ph}$ is the low energy photon energy distribution described in the last section. The equation for electrons, positrons and neutrinos can be written in a similar way, using the corresponding distribution function.

The results for secondary diffuse neutrinos are shown in figure 3. For this calculation the proton flux is normalized to scenario B, leading to a maximum neutrino flux, due to the observed photon limits by AUGER. The flux seems to be too low for detection by operating or upcoming neutrino detectors. The sensitivity for IceCube is shown for one year of operation, so there might be a chance to detect a LSC neutrino anisotropy for a longer observation time.

While the neutrinos are traveling almost unchanged from the location of their production to the detectors on Earth, electrons and photons are producing electromagnetic cascades with the same low ambient photon fields described in the last section. The few remaining direct high energy photons and the photons from the Compton-pair cascades lead to a spectrum with two distinct maxima. The maximum at low energies lies around 10^{12} to 10^{13} eV where the absorption due to the cosmic microwave background is not important any more.

The result using scenario A and B for the cosmic ray flux normalization is shown as thick solid and thick dashed line in figure 4, respectively. The data at GeV energies are the diffuse background flux detected by EGRET. The H.E.S.S. upper limit has been derived using the cosmic ray electron flux from [7]. Electromagnetic showers from photons and electrons are very similar and hard to separate. The cosmic ray electron flux still contains some amount (<50%) of photons and is therefore taken as photon upper limit. Since the spectral shape of the photon and electron distribution will be quite different we only show one point. The Milagro data point is the detected galactic diffuse gamma-ray flux. We show it as upper limit assuming that an extragalactic background flux in the same order of magnitude would have been detected by the observatory. The AUGER data points are limits on the diffuse photon flux by [8]. The diffuse sensitivities labeled with SCORE belong to a new large-area (10km^2) wide-angle (1sr) air Cherenkov detector which is under study right now. With a possible energy range of 10 TeV to 1 EeV is would close the last remaining window in gamma-ray astronomy. For more details see [9].

Note that the theoretical flux is plotted per steradian assuming that the super galactic plane covers about 1/6 of the total sky. For a more detailed treatment the

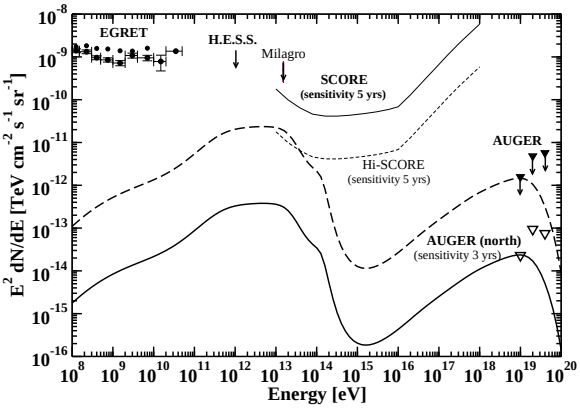

Fig. 4. Diffuse photon flux from the LSC as a function of photon energy. The thick solid line shows the minimum flux for scenario A, while the dashed is multiplied by a factor of about 100 to match the photon upper limit by AUGER in scenario B. The data and sensitivities are discussed in the text.

exposure and observation time on the super galactic plane of each instrument has to be taken into account.

V. Discussion and Conclusion

Our first estimate assuming a homogeneous, isotropic model for all particles involved leads to an anisotropy in the observed sky.

The total proton energy density used for the conservative scenario A, which is normalized to the AUGER proton spectrum at 10^{19} eV, is $u_{\rm UHCR} = 4 \times 10^{-18}$ erg cm^{-3}. This leads to an equipartition magnetic field of $B_{eq} = 10$ nG, while the upper limit, where a proton energy density higher by a factor of 100 is used, would result in$B_{eq} = 100$ nG.

The exact shape and integrated flux of the spectrum depends on several parameters. A detailed study will be done in an upcoming publication. The main parameter is the distance of the photon source. The further away the more photons are involved in the cascade which shifts more energy down into the TeV range. Therefore it is relevant if the cascades are calculated from a single gamma-ray source or from a diffuse emission all along the way through the LSC. We used the dint routine [10] which is also used in the CRPropa code [11] which can treat both point sources and diffuse sources. We found that in our case where the ultra high gamma-ray emission is truly diffuse, the actual path length plays a minor role for the cascades. This is very clear since a longer path length only adds cascades from further away while the main contribution by local emission stays the same. The direction of the integrated path length has no influence in our approximations, since the cosmic-ray density and the photon density is assumed to be homogeneous throughout the LSC.

The still missing process of (Bethe-Heitler) pair production will lead to more electron positron pairs which will enrich the cascade and therefore lead to more emission around 10^{13} eV. For steep spectral indices > 2.7 this process can dominate secondary photon production.

Another important parameter is the spectral index of the primary proton spectrum. If normalized to the same total cosmic ray density a flatter spectrum leads to more photons and secondary particles at 10^{19} eV compared with the peak at 10^{13} eV. This will enhance the ultra high energy flux and makes a detection with AUGER even more promising.

Cosmological populations of objects outside the LSC like AGN, galaxies or clusters produce an diffuse photon flux as extragalactic gamma-ray background [12]. But one has to keep in mind that the absorption due to photon photon pair production is much larger for these sources. Therefore we can say that above the pair production threshold the gamma-ray fluxes are completely dominated by the LSC, whereas at lower energies, sources at larger, cosmological distances will dominate. The diffuse, cosmological fluxes at these lower energies have been discussed, e.g. in [13]

In figure 4, we show sensitivities for AUGER north from [14] who calculated the sensitivity for the photon fraction. Their sensitivity curve has been used to calculate for three different energies the possible photon limits based on the observed cosmic-ray photon flux. The photon fractions used here are 0.03%, 0.1% and 0.4% for 10 EeV, 20 EeV and 40 EeV respectively. Even for the conservative assumption of homogeneous energy density of cosmic rays in scenario A AUGER north might be able to observe an enhanced flux from the super galactic plane.

References

[1] The Pierre Auger Collaboration; Abraham et al. Astropart. Phys. **29** (2008) 188, (ERRATUM (2008), APh, 30, 45)
[2] Globus, N., Allard, D. & Parizot, E., A & A, **479**, 97 (2008)
[3] Kneiske, T.M., Mannheim, K. & Hartmann, D.H., A & A, **386**, 1 (2002)
[4] Cole et al. MNRAS, **326**, 255, 2001
[5] Bell, E. F., McIntosh, D. H., Katz, N. & Weinberg, M. D. ApJS, **149**, 289 (2003)
[6] Kelner, S. R.& Aharonian, F. A. Phys. Rev. D **78**, 4013 (2008)
[7] Aharonian et al. Phys. Rev. L **101**, 1104, (2008)
[8] Pierre AUGER Collaboration; Abraham et al. Astropart. Phys. **29**, 243 (2008)
[9] Tluczykont, M., Kneiske T.M., Hampf, D. & Horns, D. Proceedings of the 31^{st} ICRC, Łódź 2009
[10] S. Lee, Phys. Rev. D **58**, 043004 (1998) [arXiv:astro-ph/9604098].
[11] E. Armengaud, G. Sigl, T. Beau and F. Miniati, Astropart. Phys. **28**, 463 (2007) [arXiv:astro-ph/0603675].
[12] Kneiske, T.M. ChJAS, **8**, 219 (2008)
[13] O. E. Kalashev, D. V. Semikoz and G. Sigl, Phys. Rev. D **79**, 063005 (2009) [arXiv:0704.2463 [astro-ph]].
[14] Risse, M. & Homola, P. Mod. Phys. Lett. A **22**, 749, (2007)
[15] Becker, J. K. Journal of Phys. Conf. Ser. **136**, 2055 (2008)